Electrophoretic Deposition of CdSe/ZnS Quantum Dots for Light-Emitting Devices

*Katherine W. Song, Ronny Costi, and Vladimir Bulović**

Quantum-dot light-emitting devices (QD-LEDs)[1–4] could form the foundation of the next generation of lighting and display technologies, due to the unique optical properties of colloidally synthesized quantum dots (QDs). Thin QD films have been shown to exhibit high brightness, a broad excitation spectrum, and a narrow emission bandwidth that is tunable over the entire visible spectrum; under electrical excitation, they have been shown to yield QD-LEDs of highly saturated color.[5] The most efficient QD-LEDs demonstrated to-date are fabricated by spin-casting colloidal QD solutions into QD films of controllable and uniform thickness, yielding QD-LEDs with external quantum efficiencies (EQE) above 18%.[6,7] Contact printing of QD films has also been used to fabricate patterned QD-LEDs with features on the scale of 25 μm, as would be needed for high-resolution pixelated multicolor light emitters.[8] More simply, colloidal solutions of QDs can be ink-jet printed to generate patterned luminescent films, with the benefit of high utilization of the starting material but with the tradeoff of lower resolution of the resulting features and less thickness uniformity.[9,10] In the present study, we investigate an alternative method for the large-area deposition of luminescent QD films by demonstrating electrophoretic deposition (EPD)[11–14] of QD thin films from electrostatically assembled colloidal QD solutions.

The EPD of QD thin films is accomplished by applying a voltage between two conductive electrodes that are suspended in a colloidal QD solution. The electric field established between the electrodes drives the QD deposition onto the electrodes. The benefit of EPD as a manufacturing process is the efficient use of the starting colloidal QD solutions (in contrast to spin-casting, in which the majority of the used QD solution is spun off the substrate and is unrecoverable). EPD also allows parallel processing (multiple devices may be fabricated simultaneously in the same EPD bath), and it enables deposition of films onto electrodes of arbitrary size, shape, and texture, conforming the deposited film to the electrode geometry. In addition, while spin-casting QDs is a rapid film-forming process that can lead to disordered films containing QDs that are not in a mechanical equilibrium, EPD is a slower deposition process that can allow QDs to assemble and pack in a more energetically favorable structure on the surface of the substrate. Such EPD-assembled films could in turn improve LED performance and/or operating lifetime. A handful of reports on depositing QD films via EPD have been made in recent years, but all reported techniques produce thick (>100 nm) films that are unsuitable for QD-LEDs, where a QD layer of a few monolayers in thickness is required for efficient electroluminescence.[12–17] In this report, we present QD-LEDs fabricated with a thin, electrophoretically deposited QD layer in place of a spin-cast QD film.

For the QD-LEDs fabricated in this study, **Figure 1** portrays the layered device cross section (Figure 1a) and a proposed flat-band energy diagram (Figure 1b), with energy levels taken from literature.[18–21] The QDs used are colloidal CdSe/ZnS core/shell QDs capped with carboxylic acid ligands, which allow the QDs to be solution processable and improve the photoluminescence (PL) quantum yield (QY) of the QDs by reducing surface trap states and the spatial overlap in the wavefunctions of charge carriers residing on the QDs. The PL peak of the QD solutions used in this study appears at a wavelength of $\lambda = 610$ nm, and each QD-ligand complex is between 8 nm and 10 nm in diameter.

Fabrication of the QD-LEDs starts with a commercially purchased, pre-patterned indium tin oxide (ITO) electrode on a glass substrate. After the substrate is washed with solvents and cleaned with oxygen plasma exposure, a 40 nm-thick zinc oxide (ZnO) electron-transport layer is formed by spin-casting zinc acetate solution onto the substrate and annealing it at 300 °C for 5 min in air. Then, a 10 nm thick QD film is electrophoretically deposited in an EPD process, described below in detail. The samples are then transferred into a vacuum chamber (with a base pressure of 10^{-6} Torr), where a 100 nm-thick 4,4′-*N*,*N*′-dicarbazolebiphenyl (CBP) hole-transporting layer, a 10 nm-thick molybdenum oxide (MoO_3) hole-injection layer, and a 100 nm-thick aluminum (Al) anode are deposited by sequential thermal evaporation.

For control devices, a QD solution calibrated for a known end thickness is spun onto the ZnO-on-ITO/glass stack in a nitrogen ambient glovebox. For devices with an EPD QD layer, the following procedure is used: an amber glass vial, containing a 0.1 mg mL^{-1} QD solution in a 10:1 ratio chloroform:acetonitrile solution, is placed into a sonication bath. The addition of acetonitrile partially removes passivating ligands surrounding the QDs, thus allowing surface traps on the QD to be affected by the electric field. Without the addition of acetonitrile, the EPD rate of QDs on the electrodes is greatly diminished. This observation is consistent with the measurement of electrical current through the EPD setup: the current with QDs and no acetonitrile is comparable to the current observed when only chloroform (without QDs) is present; the current in the presence of acetonitrile, on the other hand, is approximately one order of magnitude higher. An excess of acetonitrile (and/or other solvents, such as acetone) causes QDs to aggregate and

K. W. Song, Dr. R. Costi, Prof. V. Bulović
Organic and Nanostructured Electronics Laboratory
Department of Electrical Engineering and Computer Science
13-3138, Massachusetts Institute of Technology,
Cambridge, MA, 02139, USA
E-mail: bulovic@mit.edu

DOI: 10.1002/adma.201203079

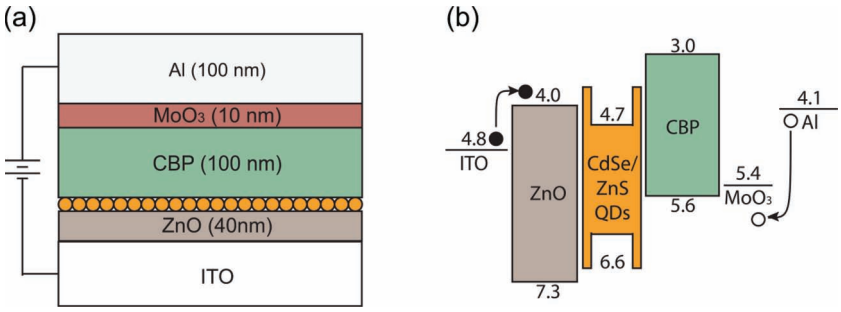

Figure 1. a,b) Cross-section schematic (a) and flat band energy diagram (b) of a QD-LED showing the device layers. The indicated band energies are in units of eV and are all referenced to the vacuum level.

crash out of solution, leading to thick films composed of large QD agglomerates.

To start the EPD process, two ZnO-on-ITO/glass substrates are secured 0.4 cm apart with their conductive sides parallel and facing toward one another, as illustrated in **Figure 2**a. An electric field in the range of 25–50 V cm^{-1} is then applied, and the electrodes are placed into the QD solution. After a fixed time (a few minutes in duration), the electrodes are lifted out of the QD solution and, with the voltage bias remaining on, washed by dipping into a vial filled with neat chloroform for 15 s. This washing step removes aggregates and QDs that are not well bound to the surface, as well as QD-rich chloroform droplets that would leave uneven QD deposits behind upon drying. The EPD procedure is performed in air. After the EPD of the QD film is complete, the samples are transferred to a nitrogen ambient glovebox and remain in an oxygen-free environment for the remainder of the fabrication process.

An atomic force microscopy (AFM) topography image of an EPD QD film on a ZnO-on-ITO anode is shown in Figure 2b. The EPD process lasted 5 min in a QD solution, with a 15 s rinse in chloroform, all under a 20 V applied bias (corresponding to an electric field of 50 V cm^{-1}). The resulting QD film roughness is 2.3 nm, which is slightly greater than the 1.5 nm roughness of the underlying ZnO-on-ITO substrate. The thickness of the QD film is measured by taking an AFM cross section of a step scratched into the QD film and is found to be 15 nm, or between 1 and 2 monolayers (Figure 2c). Under ultraviolet light, fluorescence of the QD films can be observed by eye on both the positive and negative electrodes. However, the film on the positive electrode appears brighter, suggesting that more luminescent dots are attracted to the positive electrode during deposition.

Current–voltage and external quantum efficiency (EQE) characteristics for a completed EPD QD-LED, along with those of a control spin-cast QD-LED device, are shown in **Figure 3**. A 10 nm QD film is spun on for the control device to match the thickness of the electrophoretically deposited films closely and thus provide the most relevant reference for comparison. The EPD device shown uses an anodic electrophoretically deposited QD film, and the deposition is carried out for 5 min under an applied potential of 10 V (25 V cm^{-1} electric field). The EPD QD-LED exhibits a turn-on voltage of 1.8 V, a value that is lower than the 2 V expected, given the 2.0 eV optical bandgap of the dots, and the control device has a turn-on voltage of 2.1 V. The peak EQE of the EPD QD-LED and the control device is 1.5% and 1.6%, respectively. The peak power efficiencies are 1.79 lm W^{-1} for the EPD QD-LED and 1.80 lm W^{-1} for the control QD-LED. The EPD and control devices reach 100 cd m^{-2}, the luminance value often taken as "video brightness" in the literature, under applied voltages of 4.7 V and 4.9 V, respectively, when their EQEs are 1.54% and 1.44%, respectively.[23] Inset in Figure 3b is a photograph of 10 EPD QD-LEDs (dimensions: 1.7 mm × 0.7 mm) operating simultaneously at video brightness in the dark.

The EPD QD-LEDs with the highest EQE in each fabrication batch are consistently the ones with the anodic EPD electrodes. Devices with cathodic EPD electrodes demonstrate EQEs on the order of 0.1%, and "dipped" devices, where no bias is applied while performing the same EPD procedure, achieve EQEs no higher than 0.5%. We note that the optimal combination of parameters – applied voltage and time of deposition – for which the highest device EQE is achieved varies between runs. We attribute this to a high degree of sensitivity to factors that are not controlled in our experimental setup, such as temperature, humidity, and inadvertent impurities in the solutions used for the deposition processes. In a study by Islam et al., it was shown that the presence of impurities (including free ligands) in the solution of electrophoretically deposited 0.5 μm-thick CdSe nanocrystal films greatly affects nanocrystal aggregation and adhesion to the electrode.[13] This impurity-induced variation in film morphology

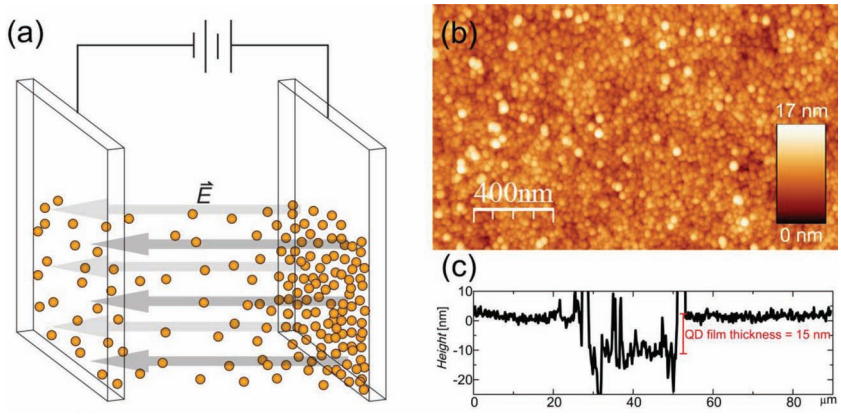

Figure 2. a) Schematic depiction of the electrophoretic deposition process. A voltage applied between two parallel, conducting electrodes spaced 0.4 cm apart drives the deposition of the particles (QDs). b) AFM topography image (using WSxM software[22]) of the surface of an electrophoretically deposited QD film with RMS roughness of 2.3 nm. This film is formed during a 5 min, 50 V cm^{-1} anodic deposition from a 0.1 mg mL^{-1} QD solution and is followed by a chloroform rinse. c) AFM cross sectional profile over a scratch in the QD film, showing a film thickness of 15 nm.

ADVANCED MATERIALS
www.advmat.de

www.MaterialsViews.com

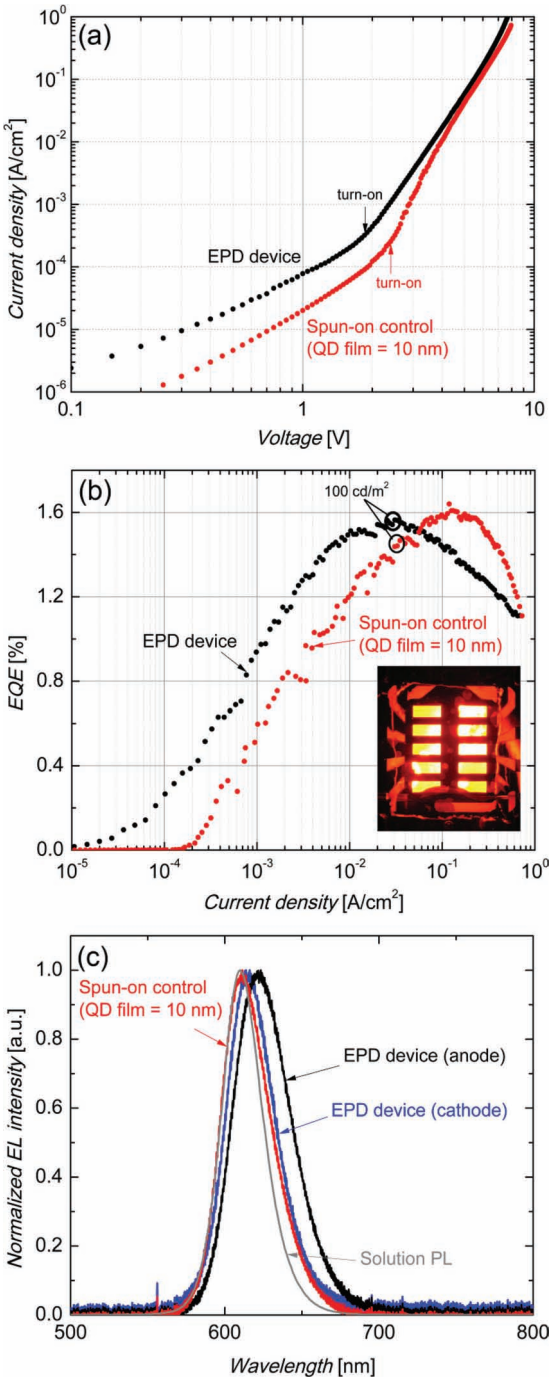

Figure 3. a,b) Current density vs. applied voltage characteristics (a) and external quantum efficiency (EQE) vs. current density (b) of a QD-LED containing an electrophoretically deposited QD film (black) and a QD-LED with a 10 nm spun-on QD film (red), showing an early turn-on voltage of 1.8 V and a 1.5% EQE for the EPD device. Inset: 10 EPD QD-LEDs (each 1.7 mm × 0.7 mm in size) operating simultaneously in the dark at ≈100 cd m^{-2}. The EPD film was formed by a 5 min, 25 V cm^{-1} anodic deposition. c) Electroluminescence (EL) spectra for EPD and spun-on QD-LEDs, where the EPD devices display red-shifts in comparison to the spun-on sample. The full-width half-maximum (FWHM) of the anodic EPD QD-LED is 16% wider than the cathodic EPD and the spun-on devices. The solution photoluminescence (PL) spectrum is also shown for reference.

is very likely present in our setup and would indeed, in turn, cause a variation in the QD-LED performance.

Figure 3c shows electroluminescence (EL) spectra for EPD and spun-on devices measured at video brightness, as well as the photoluminescence (PL) spectrum for the QDs in solution for reference. The EL peak for the anodic EPD device with characteristics plotted in Figure 3 appears at $\lambda = 623$ nm, which is red-shifted from the EL peak of the spun-on control device by 12 nm. The full width at half maximum (FWHM) of the EL peak of the anodic EPD device is 45 nm, which is 7 nm broader than that of the control. In contrast, the red-shift seen in cathodic EPD devices, as well as "dipped" devices, is only 5 nm with no significant broadening. This red-shift can be attributed to a denser QD film which would exhibit a solvatochromic red-shift.[24] Alternatively, the red-shifted emission might originate from QD agglomerates that could form in the presence of acetonitrile even before their deposition onto the electrodes.[25] Finally, it is possible that the anodic EPD process forms a permanent electric dipole layer at the interface with the ZnO film, which would affect the QDs via the electric-field-induced Stark shift. A better understanding of this effect will require further studies.

In summary, we demonstrate a new application of EPD to deposit thin, uniform CdSe/ZnS colloidal QD films a few monolayers in thickness. We show that the films formed by this EPD technique are of high optical quality, as they enable us to fabricate, for the first time, bright and efficient QD-LEDs. The EQEs of EPD-fabricated QD-LEDs are comparable to those of conventional QD-LEDs containing spun-on QD films. The turn-on voltage of the EPD-fabricated QD-LEDs corresponds to electron energies that are, surprisingly, lower than the QD optical bandgap. The results of this first study on EPD QD-LEDs indicate that EPD is a viable alternative to spin-casting in the fabrication of QD optoelectronic structures.

Acknowledgements

The authors would like to acknowledge QD Vision Inc. for supplying the QD solutions used in this study, as well as Yasuhiro Shirasaki and Geoffrey Supran for helpful discussions. We gratefully acknowledge funding by the DOE Excitonics Center at MIT, an Energy Frontiers Research Center funded by the US Department of Energy, Office of Basic Energy Sciences under award number DE-SC0001088. K.W.S. also acknowledges support from MIT School of Engineering's Henry Ford II Fellowship.

Received: July 28, 2012
Revised: September 28, 2012
Published online: December 27, 2012

[1] C. B. Murray, D. J. Norris, M. G. Bawendi, *J. Am. Chem. Soc.* **1993**, *115*, 8706–8715.
[2] B. O. Dabbousi, J. Rodriguez Viejo, F. V. Mikulec, J. R. Heine, H. Mattoussi, R. Ober, K. F. Jensen, M. G. Bawendi, *J. Phys. Chem. B* **1997**, *101*, 9463–9475.
[3] P. O. Anikeeva, J. E. Halpert, M. G. Bawendi, V. Bulović, *Nano Lett.* **2007**, *7*, 2196–2200.
[4] S. Coe-Sullivan, W. Woo, M. G. Bawendi, V. Bulović, *Nature* **2002**, *420*, 800–803.
[5] P. O. Anikeeva, J. E. Halpert, M. G. Bawendi, V. Bulović, *Nano Lett.* **2009**, *9*, 2532–2536.

[6] S. A. Coe-Sullivan, Z. Zhou, Y. Niu, J. Perkins, M. Stevenson, C. Breen, P. T. Kazlas, J. S. Steckel, *SID Int. Symp. Dig. Tech. Pap.* **2011**, *42*, 135–138.
[7] S. Coe-Sullivan, *presented at SID Display Week 2012 (Seminar M-5),* Boston, MA, June, **2012**.
[8] L. Kim, P. O. Anikeeva, S. A. Coe-Sullivan, J. S. Steckel, M. G. Bawendi, V. Bulović, *Nano Lett.* **2008**, *8*, 4513–4517.
[9] V. Wood, M. J. Panzer, J. Chen, M. S. Bradley, J. E. Halpert, M. G. Bawendi, V. Bulović, *Adv. Mater.* **2009**, *21*, 2151–2155.
[10] M. J. Panzer, V. Wood, S. M. Geyer, M. G. Bawendi, V. Bulović, *IEEE J. Disp. Tech.* **2010**, *6*, 90–93.
[11] O. O. van der Biest, L. J. Vandeperre, *Annu. Rev. Mater. Sci.* **1999**, *29*, 327–352.
[12] M. A. Islam, I. P. Herman, *Appl. Phys. Lett.* **2002**, *80*, 3823–3825.
[13] M. A. Islam, Y. Q. Xia, D. A. Telesca, M. L. Steigerwald, I. P. Herman, *Chem. Mater.* **2004**, *16*, 49–54.
[14] P. Brown, P. V. Kamat, *J. Am. Chem. Soc.* **2008**, *130*, 8890–8891.
[15] N. J. Smith, K. J. Emmett, S. J. Rosenthal, *Appl. Phys. Lett.* **2008**, *93*, 043504.
[16] S. Ameen, M. S. Akhtar, S. G. Ansari, O.-B. Yang, H.-S. Shin, *Superlattices Microstruct.* **2009**, *46*, 872–880.
[17] A. Salant, M. Shalom, I. Hod, A. Faust, A. Zaban, U. Banin, *ACS Nano* **2010**, *4*, 5962–5968.
[18] S. Tokito, K. Noda, Y. Taga, *J. Phys. D: Appl. Phys.* **1996**, *29*, 2750–2753.
[19] G. E. Jabbour, Y. Kawabe, S. E. Shaheen, J. F. Wang, M. M. Morrell, B. Kippelen, N. Peyghambarian, *Appl. Phys. Lett.* **1997**, *71*, 1762–1764.
[20] I. G. Hill, A. Kahn, *J. Appl. Phys.* **1999**, *86*, 4515–4519.
[21] V. Wood, M. J. Panzer, J. E. Halpert, J. M. Caruge, M. G. Bawendi, V. Bulović, *ACS Nano* **2009**, *3*, 3581–3586.
[22] I. Horcas, R. Fernandez, J. M. Gomez-Rodriguez, J. Colchero, J. Gomez-Herrero, A. M. Baro, *Rev. Sci. Instrum.* **2007**, *78*, 013705.
[23] H. Sirringhaus, N. Tessler, R. H. Friend, *Science* **1998**, *280*, 1741–1744.
[24] C.A. Leatherdale, M. G. Bawendi, *Phys. Rev. B* **2001**, *63*, 165315.
[25] C. R. Kagan, C. B. Murray, M. Nirmal, M. G. Bawendi, *Phys. Rev. Lett.* **1996**, *76*, 1517–1520.